ORIGINAL ARTICLE

Canagliflozin protects the cardiovascular system through effects on the gut environment in non-diabetic nephrectomized rats

Ayumi Matsui[1] · Ayumi Yoshifuji[1] · Junichiro Irie[1,2] · Takaya Tajima[1] · Kiyotaka Uchiyama[1] · Tomoaki Itoh[1] · Shu Wakino[1] · Hiroshi Itoh[1,2]

Abstract

Background The gut produces toxins that contribute to the cardiovascular complications of chronic kidney disease. Canagliflozin, a sodium glucose cotransporter (SGLT) 2 inhibitor that is used as an anti-diabetic drug, has a weak inhibitory effect against SGLT1 and may affect the gut glucose concentration and environment.

Methods Here, we determined the effect of canagliflozin on the gut microbiota and the serum gut-derived uremic toxin concentrations in 5/6th nephrectomized (Nx) rats.

Results Canagliflozin increased the colonic glucose concentration and restored the number of *Lactobacillus* bacteria, which was low in Nx rats. In addition, the expression of tight junction proteins in the ascending colon was low in Nx rats, and this was partially restored by canagliflozin. Furthermore, the serum concentrations of gut-derived uremic toxins were significantly increased by Nx and reduced by canagliflozin. Finally, the wall of the thoracic aorta was thicker and there was more cardiac interstitial fibrosis in Nx rats, and these defects were ameliorated by canagliflozin.

Conclusions The increases in colonic glucose concentration, *Lactobacillus* numbers and tight junction protein expression, and the decreases in serum uremic toxin concentrations and cardiac interstitial fibrosis may have been caused by the inhibition of SGLT1 by canagliflozin because similar effects were not identified in tofogliflozin-treated rats.

Keywords Canagliflozin · Chronic kidney disease · Gut microbiota

Introduction

The number of patients with chronic kidney disease (CKD) is increasing alongside the aging of the population and the increases in the prevalence of hypertension and diabetes. However, conventional therapies for CKD, such as blood pressure control and a low-protein diet, are not sufficient to stop the progression of CKD. Recently, there has been growing interest in the gut as a therapeutic target of CKD. Colonic bacteria are the principal source of several uremic toxins and that the composition of the intestinal microbiome differs in CKD [1–3]. In particular, larger numbers of intestinal bacteria that express urease and uricase and produce indole or *p*-cresol have been demonstrated in patients with end-stage renal disease (ESRD) [4]. Because most of the colon microbiota-derived uremic toxins are nephrotoxic, as well as having cardio-toxic effects, the dysbiosis that characterizes CKD might contribute to the progression of renal failure and the incidence of cardiovascular events [5–8].

Previous study showed that there is a larger population of *Bacteroides* and a smaller population of *Lactobacillus* species in 5/6th nephrectomized (Nx) rats, which leads to dysfunction of their intestinal epithelial barrier [9–11]. This can be explained by the ability of *Lactobacillus* species to maintain the expression of tight junction (TJ) proteins [12], which limits the accumulation of uremic toxins in the serum of patients or animals with CKD. Therefore, a therapeutic strategy that corrects this dysbiosis may be clinically useful, and several kinds of prebiotic and probiotic therapies have been tested for reno-protective or cardio-protective effects in animal models of and patients with CKD [13–15].

✉ Shu Wakino
shuwakino@z8.keio.jp

1 Department of Internal Medicine, School of Medicine, Keio University, 35 Shinanomachi, Shinjyuku-Ku, Tokyo 160-8584, Japan

2 AMED-CREST, Japan Agency for Medical Research and Development, Tokyo, Japan
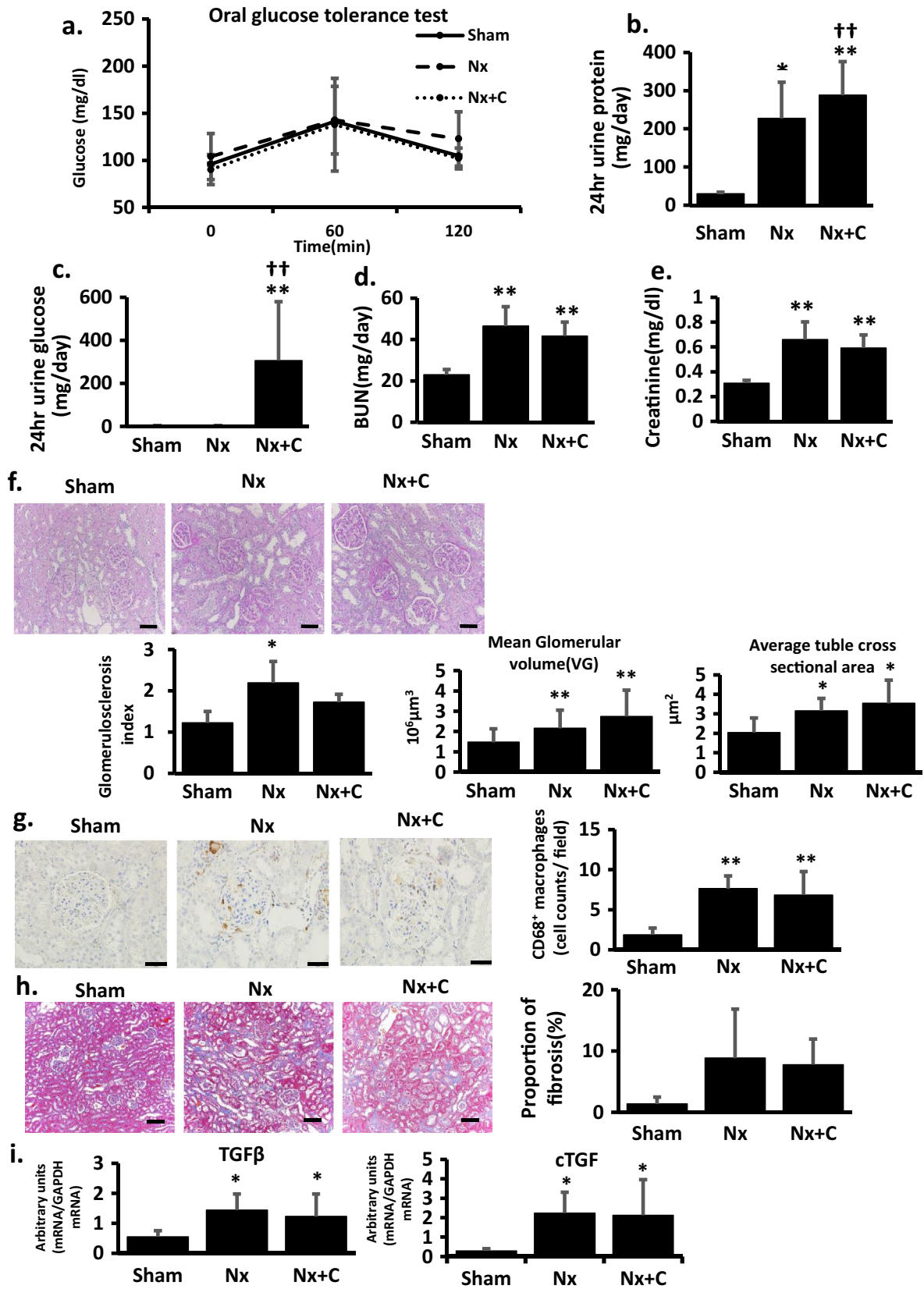
◄**Fig. 1** Effect of canagliflozin on biochemical parameters and kidney function. **a** Results of oral glucose tolerance testing. **b**, **c** Effect of canagliflozin on 24-h urinary protein excretion of protein (**b**) and glucose (**c**). **d**–**e** Effect of canagliflozin on blood urea nitrogen (BUN, **d**) and serum creatinine (**e**). **f** The representative images of periodic acid-Schiff-stained kidney sections in each rat group. The bar graphs in the lower panel represented the glomerulosclerotic index (left), the sizes of glomerulus (middle), and those of tubules (right) of each group. Scale bars: 100 μm. **g** Infiltrated macrophages in the kidney of each group was immune-stained with CD68 antibody. The bar graph in the right panel showed the quantification of CD68-positive cells in each group. Scale bars: 50 μm. **h** Representative cortical tubulo-interstitial images (upper panel) and quantitative analysis (lower panel) of Masson's trichrome-stained kidney sections. Scale bars: **h** 100 μm and (i) 200 μm. (i) Renal *Tgfb1* and *Ctgf* mRNA expression. Nx; Nephrectomized rats, Nx + C; canagliflozin-treated Nx. *$p < 0.05$, **$p < 0.01$ versus the Sham group; ††$p < 0.05$ versus the Nx group ($n = 12$ per group)

In the present study, we aimed to determine whether the anti-diabetic drug canagliflozin, which is a sodium glucose cotransporter (SGLT) 2 inhibitor, has prebiotic effects. SGLT2 inhibitors reduce the blood glucose concentration by inhibiting glucose reabsorption in kidney tubules and promoting glucose excretion in the urine. There are six isoforms of SGLT, and SGLT2 is predominantly expressed in the renal proximal tubule, whereas SGLT1 is expressed in small intestinal epithelial cells, where it plays a major role in intestinal glucose absorption. Canagliflozin differs from other SGLT2 inhibitors in that it weakly inhibits SGLT1, and it therefore might affect the gut environment. An in vitro comparison of the six different clinically available SGLT2 inhibitors in SGLT-overexpressing cells showed that canagliflozin had a 290-fold selectivity for SGLT2 *vs.* SGLT1 (the lowest selectivity), whereas that of tofogliflozin was 2900 (the highest selectivity) [16]. In another study, the inhibition constants (Ki) for SGLT1 and SGLT2 were 770.5 and 4.0 nM, respectively [17]. The Ki value for SGLT1 suggests that canagliflozin inhibits SGLT1 in the small intestine from the luminal side. Therefore, we hypothesized that canagliflozin might affect the dysbiosis of animals with CKD, and thereby influence renal or cardiovascular function. In the present study, we aimed to determine the effects of canagliflozin on the gut microbiota and uremia of non-diabetic rats with CKD, and to determine whether it has a protective effect on the cardiovascular system.

Materials and methods

Animal care and experiments

Six-week-old, male, spontaneously hypertensive rats (Charles River, Wilmington, MA, USA) were randomly assigned to three experimental groups: a sham-operated group, an Nx group, and an Nx + C group, which was administered 0.024% canagliflozin in standard chow (Mitsubishi Tanabe Pharma Corporation, Osaka, Japan). We also conducted a study using another SGLT2 inhibitor, tofogliflozin. In this study, 6-week-old, male rats were assigned to the same three groups, plus a fourth Nx + T group, which was administered 0.015% tofogliflozin in standard chow (Kowa Pharmaceutical Co. Ltd., Montgomery, AL, USA). The doses of canagliflozin and tofogliflozin used were based on a previous study which showed that these were the doses required to significantly increase urinary glucose excretion and reduce blood glucose concentration in diabetic animals [18–20]. We also confirmed that the administration of each drug generated a similar plasma glucose curve during OGTT (Fig. 1a and 4a). Nephrectomy was performed as previously described [21]. At 17 weeks of age, OGTT was performed by orally administering 2 g/kg of glucose solution after overnight fasting, then measuring the blood glucose concentrations of the rats 0, 30 60, and 120 min later using a blood glucose meter (One Touch UltraVue, Johnson and Johnson, New Brunswick, NJ, USA). On the day following OGTT, the rats were housed in individual metabolic cages for 24 h to determine their daily urine output and food intake. The following week, their body masses and systolic blood pressures were measured, then they were terminally anesthetized. The colon of each was removed to measure their glucose contents, and samples were snap-frozen in liquid nitrogen for subsequent measurements. The kidneys, thoracic aorta, and the remaining half of the heart were sliced transversely and fixed in 10% formalin solution for tissue sectioning.

Measurement of the intestinal glucose content

Intestinal glucose content was measured as previously described [22]. Briefly, the contents of the colon were collected using 5 ml ice-cold saline and the volume was measured. The carbohydrates in the collected sample were hydrolyzed by boiling in H_2SO_4, then the mixture was neutralized using NaOH. The glucose content was then measured using a kit (LabAssay Glucose, Fujifilm Wako Pure Chemical Industries, Osaka, Japan).

Physiological and biochemical analyses

Systolic blood pressure was measured using the tail-cuff method (Model MK-1030, Muromachi Kikai, Tokyo, Japan). Urinary protein excretion was measured using the pyrogallol red method and urinary glucose excretion using the hexokinase method. The serum concentration of creatinine was measured using the creatininase-creatinase-Sarcosine oxidase-Peroxidase method. BUN was measured using the urease method. The serum concentrations of IS, PCS, HA, and IAA were measured by high-performance liquid chromatography as previously described [23].

Histological examination

Kidney sections were stained using periodic acid-Schiff to assess glomerular sclerosis and using Masson's trichrome to assess interstitial fibrosis. Glomerulosclerosis was evaluated by counting sclerotic glomeruli and calculating the glomerulosclerotic index [24, 25]. The proportion of the area of each kidney section that was fibrotic was measured using ImageJ software (NIH, Bethesda, MD, USA). The thickness of the aortic wall was determined on hematoxylin and eosin-stained sections by obtaining digital images (Upright optical microscope BX53, Olympus, Tokyo, Japan) We evaluated the thickness of aortic wall at the base of aortic arch of each rat. We measured five different places per each aortic wall using Image J. The mean value was considered to be representative for each rat. The myocardium was stained using Picrosirius red and the proportion of the area on each section that was stained red was measured using Image J and used as a measure of the degree of fibrosis. Immunohistochemistry was performed as described previously [12] using primary antibodies against CD68 (1:500, abcam plc., Cambridge, UK), Claudin-1 (1:50, Thermo-Fisher Scientific, Waltham, MA, USA/ Rockford, IL, USA), and ZO-1 (1:750, Thermo-Fisher Scientific, Waltham, MA, USA/ Rockford, IL, USA). Horseradish peroxidase-conjugated anti-rabbit IgG antibodies (Dako, Glostrup, Denmark) were used as secondary antibodies (Table 1).

Analysis of the gut microbiota

Fecal samples were suspended in 4 M guanidium thiocyanate, 100 mM Tris–HCl (pH 9.0), and 40 mM EDTA, and then homogenized using zirconia beads (5 m/s, 5 min) and a FastPrep FP100A instrument (MP Biomedicals, Santa Ana, CA, USA). DNA was extracted from the homogenates using a GC series Genomic DNA Whole Blood kit (Precision System Science, Chiba, Japan). After adjusting the final concentration of the extracted DNA to 10 ng/μl, fecal 16S rDNA was amplified by PCR. The primers used were 6-FAM-labeled 516f (5′-TGCCAGCAGCCGCGGTA-3′) and 1510r (5′-GGTTACCTTGTTACGACTT-3′). The amplified DNA was verified by electrophoresis and purified using a MultiScreen FB filter plate (Millipore, Bedford, MA, USA). The abundance of specific bacterial groups in the rat fecal samples was measured by real-time quantitative PCR using the 7500 Fast Real-time PCR System (Applied Biosystems, Foster City, CA, USA). The specific primers for *Lactobacillus* and *Bacteroides* species are shown in Table 2. The results obtained using the specific primers were normalized to those obtained using the universal primers.

FITC-dextran test and D-xylose test

Intestinal macromolecular permeability and the intestinal absorptive capacity were tested. For this purpose, a solution of fluorescein isothiocyanate (FITC)-Dextran (Sigma) 750 mg/kg body weight and D-Xylose (Sigma) 0.5 g/kg body weight were prepared in distilled water at a concentration of 50 mg of D-xylose and 75 mg of FITC-dextran per milliliter. One hour after these reagents were given by garage (l ml/100 g BW) under light ether anesthesia, the rats were terminally anesthetized and serum concentrations of these reagents were measured.

Immunoblot analysis

Frozen ascending colon samples were homogenized in cold RIPA Lysis buffer (Santa Cruz Biotechnology, Dallas, TX,

Table 1 Effects of canagliflozin on physiological parameters

	Sham	Nx	Nx + C
Body weight (g)	364.7 ± 13.3	311.0 ± 42.8[**]	323.3 ± 18.8[**]
Food intake (g/day)	19.2 ± 1.9	17.1 ± 2.4	19.2 ± 0.3
Systolic blood pressure (mmHg)	168.8 ± 17.0	220.1 ± 32.8[**]	214.8 ± 22.8[**]
Daily urine volume (ml/day)	12.2 ± 3.1	29.5 ± 15.9[*]	37.4 ± 10.0[**††]

Data are presented as means ± SEMs

[*]$p < 0.05$

[**]$p < 0.01$ vs. the Sham group

[††]$p < 0.01$ vs. the Nx group

Table 2 Primers used for the quantification of bacterial genera

Bacteria	Forward	Reverse
Lactobacillus	AGCAGTAGGGAATCTTCCA	CACCGCTACACATGGAG
Bacteroides	GAAGGTCCCCCACATTG	CAATCGGAGTTCTTCGTG
Universal primers	TCCTACGGGAGGCAGCAGT	GACTACCAGGGTATCTAATCCTGTT

USA) containing protease and phosphatase inhibitors, and the homogenates were centrifuged at $12,000 \times g$ at 4 °C for 15 min. The supernatants were collected and the protein concentration of each was determined using a DC protein assay kit (Bio-Rad Laboratories, Inc. Hercules, CA, USA). Equivalent amounts of protein (50 μg) were loaded and electrophoresed on 7.5%, 10%, or 12% sodium dodecyl sulfate–polyacrylamide gel electrophoresis gels and transferred to polyvinylidene difluoride membranes. The resulting blots were incubated with primary antibodies against rat ZO-1, occludin, claudin-1 (Invitrogen, Carlsbad, CA, USA), or β-actin (Cell Signaling Technology, Danvers, MA, USA). After washing, the blots were incubated with secondary antibody (horseradish peroxidase-linked anti-rabbit IgG; GE Healthcare, Amersham, UK) and the protein–antibody complexes were detected using an ECL detection kit (Amersham Biosciences, Uppsala, Sweden), according to the manufacturer's recommended protocol.

Real-time reverse transcriptase-polymerase chain reaction

RNA was extracted from frozen cardiac tissue using an RNeasy Mini Kit (Qiagen, Hilden, Germany). Equal amounts (1 μg) of RNA from each sample were reverse-transcribed to cDNA using a Prime Script RT reagent kit with gDNA Eraser (Takara, Ohtsu, Japan). Real-time RT-PCR was then performed using the 7500 Fast Real-Time PCR System (Applied Biosystems). The primers used are shown in Table 3. Glyceraldehyde 3-phosphate dehydrogenase was used as the reference protein.

Statistical analysis

Data are presented as means ± SEMs and were analyzed using one-way analysis of variance, followed by Bonferroni's *post hoc* test. $P < 0.05$ was considered to represent statistical significance.

Results

Effects of canagliflozin on rat physiology

The Nx rats lost weight, but there was no significant difference in body mass between Nx rats and Nx rats treated with canagliflozin (Nx + C group) (Table 1). There were no significant differences in daily food intake among sham-operated, Nx, and Nx + C rats (Table 1). The Nx rats developed hypertension, unlike the sham-operated rats, but there was no difference in blood pressure between the Nx rats and Nx + C rats (Table 1). Treatment with canagliflozin significantly increased the volume of urine passed daily, compared with the Sham and the Nx rats (Table 1). These results suggest that canagliflozin induces osmotic diuresis by inhibiting SGLT2 in proximal tubular cells.

### Effects of canagliflozin on glucose tolerance, urine composition, and kidney function

Oral glucose tolerance testing (OGTT) demonstrated no significant differences in glucose tolerance among the Sham, Nx, and Nx + C groups (Fig. 1a). Nx rats developed substantial proteinuria, which was more pronounced in canagliflozin-treated rats (Fig. 1b). Canagliflozin significantly increased daily urinary glucose excretion, compared with the Sham and Nx groups (Fig. 1c). Both the blood urea nitrogen (BUN) and serum creatinine concentrations were significantly higher in Nx than Sham rats, and canagliflozin did not affect these parameters (Fig. 1d and e, respectively). In renal histology, glomerulosclerosis was evident in Nx rats, which was not altered by canagliflozin. The sizes of glomerulus and tubules were increased in Nx rats, which were not altered by canagliflozin treatment (Fig. 1f). The number of infiltrated macrophages was higher in Nx than Sham rats, and canagliflozin did not change these numbers (Fig. 1g). Nx rats showed substantial interstitial fibrosis (blue staining) that was not affected by canagliflozin treatment (Fig. 1h). Renal mRNA expressions pro-fibrotic *Tgfb1* and pro-inflammatory chemokine *Ctgf* were increased in Nx rats, which were not changed by canagliflozin treatment (Fig. 1i). These data indicate that canagliflozin does not ameliorate the glomerulosclerosis or interstitial fibrosis that characterize Nx rats.

Effect of canagliflozin on the gut microbiota and intestinal barrier

We next determined the effect of canagliflozin on the gut environment of Nx rats. The quantity of glucose per 10 cm of colon was higher in the Nx + C group than in the Sham or Nx groups (Fig. 2a), which confirms that canagliflozin inhibits SGLT1 in Nx rat colon and implies that canagliflozin might

Table 3 Primers used for real-time PCR

Gene	Forward	Reverse
TGFβ (rat)	CATTGCTGTCCCGTGCAGA	AGGTAACGCCAGGAATTGTTGCTA
CTGF (rat)	CATGGTCAGGCCCTGTGAA	CACAGAACTTAGCCCGGTAGGTC
GAPDH (rat)	GTTACCAGGGCTGCCTCTC	GGGTTTCCCGTTGATGACC
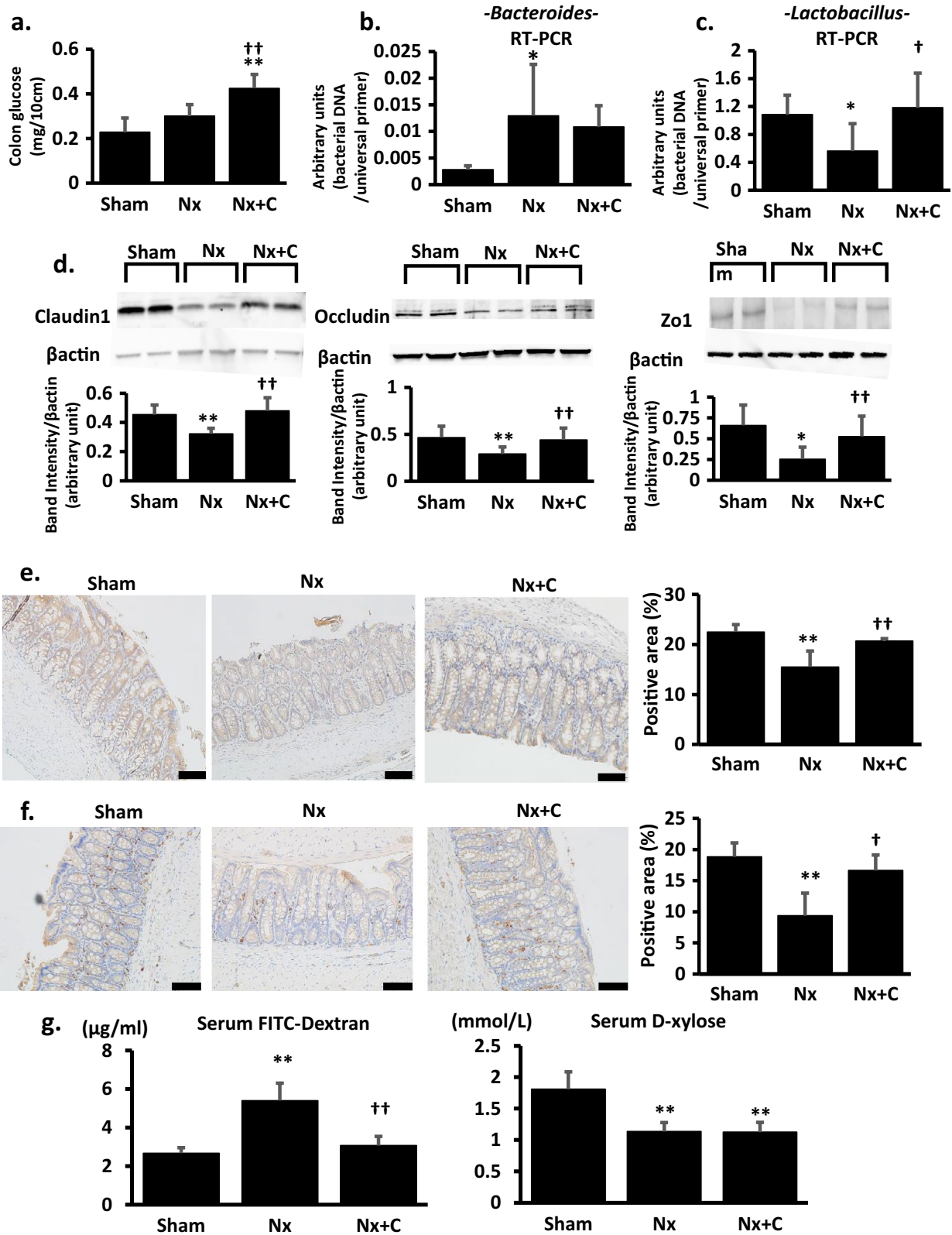
alter the composition of the microbiota in Nx rats. Quantitative analysis of the microbiota showed that *Bacteroides* species were more abundant in Nx rats and that canagliflozin had no effect on this difference (Fig. 2b). Conversely, *Lactobacillus* species were significantly less abundant in Nx rats, and this phenotype was reversed by canagliflozin treatment

◀**Fig. 2** Effect of canagliflozin on the gut microbiota and intestinal barrier. **a** Effect of canagliflozin on the colon glucose content. **b**, **c** The abundance of *Bacteroides* (**b**) and *Lactobacillus* (**c**) in the colons of rats was quantified using RT-PCR. **d** Immunoblotting showing expressions of tight junction proteins, claudin-1 (right), occludin (middle), and ZO-1 (left) in the colon. Lower panel of each blot shows the densitometric analysis of its expression. **e**, **f** Immunohistochemistry showing the expressions of tight junction proteins, claudin-1 (**e**) and ZO-1 (**f**) in the colon. Right panel of each protein shows the quantification of staining of each protein. Scale bars: 100 μm. **g** The results of FITC-Dextran (left) and D-Xylose (right) absorption test. Nx; Nephrectomized rats, Nx + C; canagliflozin-treated Nx. *$p < 0.05$, **$p < 0.01$ *versus* the Sham group; †$p < 0.05$, ††$p < 0.01$ versus the Nx group ($n = 12$ per group)

(Fig. 2c). In our previous study [12], the presence of *Lactobacillus* restored the CKD-related defect in the intestinal barrier by restoring the expression of TJ proteins. Immunoblotting analysis showed reductions in expression of both the transcellular TJ proteins claudin-1 and occludin and the cytosolic scaffold protein zonula occludens (ZO)-1 in Nx rats vs. Sham rats, and that canagliflozin restored the expression of each of these in the colons of Nx rats (Fig. 2d). Similarly, in immunohistochemical analysis, the expressions of both cludin-1 and ZO-1 were decreased in Nx rats, which were ameliorated by canagliflozin (Fig. 2e and f, respectively). Consistently, FITC-Dextran absorption test showed that the absorption of FITC-dextran was increased in Nx rats, which were ameliorated by canagliflozin treatment (Fig. 2g, right), showing the effect of canagliflozin on the colon permeability in Nx rats. On the other hand, D-Xylose absorption test revealed that the absorption of D-Xylose was decreased in Nx rats, which was not affected by canagliflozin (Fig. 2g, left).

Effects of canagliflozin on the serum concentration of uremic toxins and the cardiovascular system

Because canagliflozin affects the expression of colonic TJ proteins, we predicted that it would also affect the serum concentration of gut-derived uremic toxins. The serum concentrations of uremic toxins, such as indoxyl sulfate (IS), hippuric acid (HA), and indole acetic acid (IAA), were significantly increased by 5/6th nephrectomy (Fig. 3a), as was that of P-cresyl sulfate (PCS), but this effect did not achieve statistical significance (Fig. 3a). Although canagliflozin had no effects on the serum concentrations of PCS or IAA, it significantly reduced those of IS and HA (Fig. 3a). IS has been shown to promote aortic wall thickening and calcification and to aggravate cardiac fibrosis [26–29]. Therefore, we assessed the aortic wall thickening and cardiac fibrosis in each group. The Nx rats had significantly thicker thoracic aortic walls than the Sham rats (Fig. 3b). In addition, the extent of intestinal fibrosis, assessed using Picosirius red staining, was significantly greater in the Nx group than in the

Sham group (Fig. 3c). As shown in Fig. 3b and c, canagliflozin ameliorated both the aortic wall thickening and cardiac interstitial fibrosis. Moreover, the increases in cardiac *Tgfb1* and *Ctgf* mRNA expression in Nx rats were significantly ameliorated by canagliflozin treatment (Fig. 3d).

Effects of tofogliflozin on the glucose tolerance, urine composition, gut microbiota, intestinal barrier, and serum concentrations of uremic toxins of the rats

OGTT demonstrated no significant differences in glucose tolerance among the Sham, Nx, and tofogliflozin-treated Nx (Nx + T) groups (Fig. 4a). Tofogliflozin treatment increased urinary glucose excretion to a similar extent to canagliflozin treatment (Fig. 4b), which implies that it similarly inhibited SGLT2 in the kidney. However, because tofogliflozin has very little binding affinity for SGLT1, it failed to increase the amount of glucose in the colon compared with the Sham and Nx groups, whereas canagliflozin treatment increased the amount of glucose in the colon *vs*. the Sham, Nx, and Nx + T groups (Fig. 4c). RT-PCR for *Lactobacillus* species revealed that there was no significant difference in the abundance of these bacteria between the Nx + T group and the Nx group, but they were more abundant in the Nx + C group than in either the Nx group or the Nx + T group (Fig. 4d). Immunoblotting analysis of the rat colons showed that the expression of the TJ proteins claudin-1, occludin, and ZO-1 was lower in the Nx group. The reductions in the expression of claudin-1 and occludin appeared to be ameliorated by treatment with tofogliflozin, but these effects did not achieve statistical significance (Fig. 4e). Finally, the higher serum concentrations of IS and HA in the Nx rats were not affected by treatment with tofogliflozin (Fig. 4f).

Comparison of the effects of tofogliflozin and canagliflozin on the cardiovascular system

As described above, canagliflozin ameliorated the cardiac interstitial fibrosis that was caused by Nx. However, tofogliflozin did not have this effect (Fig. 5a). Similarly, the high *Tgfb1* and *Ctgf* mRNA expression in the hearts of the Nx rats was significantly reduced by canagliflozin, but not by tofogliflozin (Fig. 5b).

Discussion

In the present study, we have demonstrated that canagliflozin increases the glucose content of the colon and increases the abundance of *Lactobacillus* species in the microbiota of a non-diabetic rat model of CKD. This likely explains the restoration of the intestinal barrier function by canagliflozin
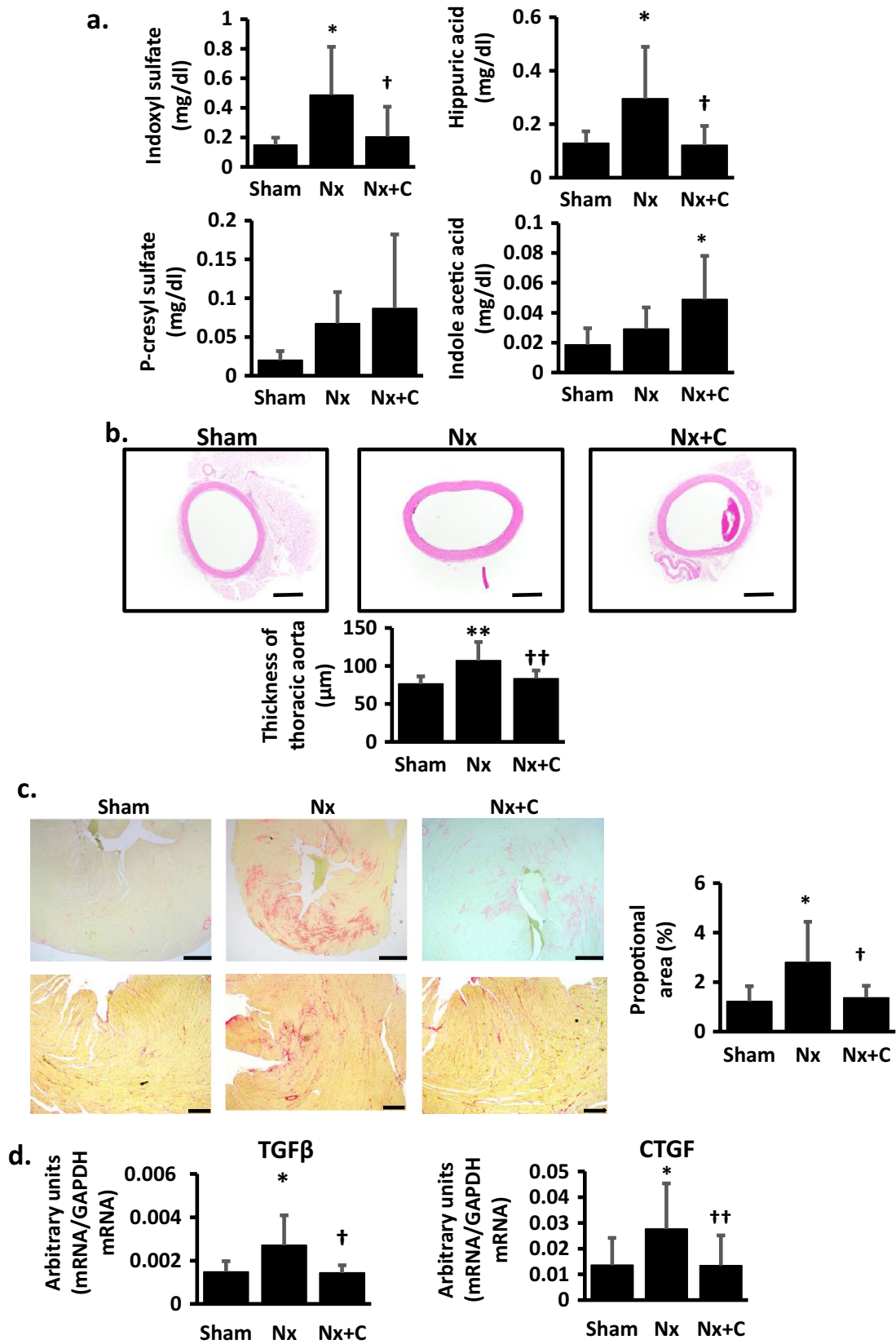
◄**Fig. 3** Effects of canagliflozin on the serum concentrations of uremic toxins and the cardiovascular system. **a** Effect of canagliflozin on the serum concentrations of indoxyl sulfate, hippuric acid, *p*-cresyl sulfate and indoxyl acetic acid. **b** Effect of canagliflozin on thickness of the thoracic aortic wall. **c** Representative images of left ventricles stained using Picrosirius red. Upper panel shows a photo of low-power field (scale bars; 1 mm) and lower panel shows a photo of high-power field (scale bars; 500 μm). The bar graph in the right side represents proportion of the myocardium that was fibrotic. **d** Effect of canagliflozin on Cardiac *Tgfb1* and *Ctgf* mRNA expression. Nx; Nephrectomized rats, Nx+C; canagliflozin-treated Nx. Scale bars: **b**, **c** 500 μm. *$p < 0.05$, **$p < 0.01$ versus the Sham group; †$p < 0.05$, ††$p < 0.01$ versus the Nx group ($n = 12$ per group)

and the reduction in the serum concentrations of IS and HA. Although canagliflozin did not affect the renal function of the rats, it ameliorated their arterial wall thickening and cardiac fibrosis. These protective effects were presumably the result of the lower serum uremic toxin concentrations. In addition, another SGLT2 inhibitor, tofogliflozin, which has a minimal effect on SGLT1, did not significantly affect the gut microbiota, expression of gut TJs, serum gut-derived uremic toxin concentrations, or the degree of cardiac fibrosis in the Nx rats. We conclude that the effects of canagliflozin on the gut microbiota, uremic toxins, and heart are independent of its glucose-lowering effects and are related to its inhibitory effects on gut SGLT1.

Canagliflozin differs from other SGLT2 inhibitors in that it weakly inhibits SGLT1 and thereby reduces postprandial intestinal glucose absorption [30]. We hypothesized that this SGLT1 inhibition might affect the uremic state. A previous study showed that phlorizin, a natural polyphenol and dietary constituent that is known to potently inhibit intestinal SGLT1, modifies the gut microbial community structure of diabetic mice [31]. Specifically, it increases the abundances of *Akkermansia muciniphila* and *Prevotella*, and this effect may be mediated through inhibition of intestinal SGLT1 [31]. Consistent with these reports, the present study demonstrated that canagliflozin but not tofogliflozin largely restores the correct proportion of *Lactobacillus* in the microbiota of CKD rats, probably through its inhibition of SGLT1. The mechanism whereby intestinal SGLT1 inhibition leads to *Lactobacillus* growth in the colon is not completely understood. However, it is thought that SGLT1 inhibition causes glucose malabsorption in the small intestine and a consequent increase in glucose delivery to the colon, which was also suggested in the present study. Because *Lactobacillus* uses glucose as a substrate for fermentation, it is likely that the higher colonic glucose concentration would stimulate the growth of *Lactobacillus*. Some previous studies have already shown that *Lactobacillus* species multiply in glucose-rich conditions [32, 33]. Furthermore, studies of prebiotics have shown that an increase in the supply of substrate leads to an increase in the population of the intestinal bacteria which metabolize that substrate [34–36]. Taking these findings

together, it can be surmised that an increase in glucose delivery to the colon stimulates an increase in the abundance of *Lactobacillus* species, which has various beneficial effects.

Lactobacillus is a well-known probiotic that is capable of reducing the serum concentrations of uremic toxins, such as PCS and IS, in patients with CKD [37–39]. We have also demonstrated that a substantial *Lactobacillus* population is associated with intactness of the intestinal barrier in CKD rats, which involves the maintenance of TJ protein expression and low serum concentrations of PCS and IS [12]. The present finding that canagliflozin, but not tofogliflozin, treatment is associated with restoration of intestinal barrier function in the same way to that shown in our previous study lead us to surmise that the maintenance of TJ expression induced by canagliflozin is the result of its effect to promote the growth of *Lactobacillus* species. However, the effect of canagliflozin administration differs from that of *Lactobacillus* administration, because it did not cause a reduction in the serum concentration of PCS. This disparity might relate to differences in the biosynthetic pathways for IS and PCS. The IS precursor indole is directly absorbed through TJs, whereas the PCS precursor *p*-cresol is conjugated to sulfate by aryl sulfotransferases at the colonic epithelium before being absorbed through TJs [3, 40, 41]. It is possible that the high concentration of glucose in the intestine that is induced by canagliflozin treatment, but that is not induced by *Lactobacillus* prebiotic treatment, might affect intestinal epithelial function. This might modify the absorption of *p*-cresol, and because HA is absorbed through TJs in a similar manner to IS [42], the serum concentration of HA was also affected by canagliflozin administration. IAA differs from the other three uremic toxins in that it is generated in part outside the gut [43, 44], which may explain the lack of effect of canagliflozin on serum IAA concentration.

It is well known that IS stimulates the progression of both tubulo-interstitial fibrosis and glomerular sclerosis in CKD by inducing reactive oxygen species (ROS) production [45, 46]. However, in the present study, canagliflozin reduced the serum IS concentration but failed to ameliorate the renal tubulo-interstitial fibrosis or glomerular sclerosis. The progression of CKD is multifactorial, involving hyperactivity of the intrarenal renin–angiotensin–aldosterone system [47], tissue hypoxia [48, 49], and high serum concentrations of uremic toxins [50–52]. Therefore, it is perhaps not surprising that a reduction in the serum IS concentration alone did not prevent the progression of CKD in the present study. Moreover, the renal damages in Nx rats are primarily due to the activation of renin–angiotensin system which leads to glomerular hypertension [53]. Since SGLT2 inhibitors including canagliflozin have hardly any direct renin–angiotensin system (RAS) inhibitory effects [54], it cannot reduce serum creatinine concentration or proteinuria in Nx rats, although, in the clinical trial, SGLT2 inhibitors have shown
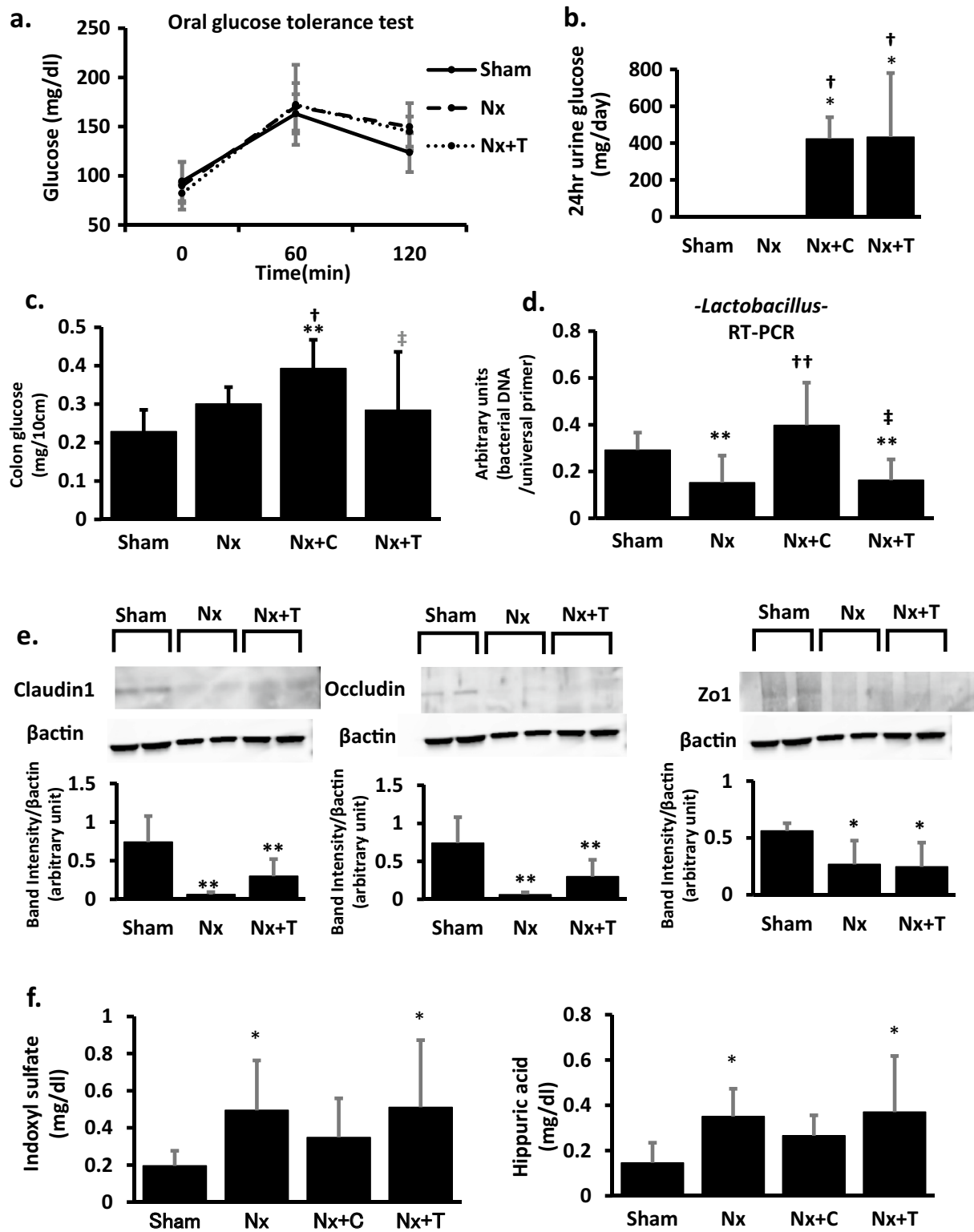
Fig. 4 Comparisons between the effects of tofogliflozin and canagliflozin. **a** The effects of tofogliflozin (T) on oral glucose tolerance testing. **b**, **c** Effect of tofogliflozin (T) and canagliflozin (C) on 24-h urinary glucose excretion (**b**) and colon glucose content (**c**). (**d**) The abundance of *Lactobacillus* in the colons of the rats. **e** Expression of the tight junction proteins claudin-1, occludin, and ZO-1 in the colon. Upper pannel shows an immunoblot of a TJ protein and lower panel shows the densitometric analysis of its expression. **f** Effect of tofogliflozin on the serum concentrations of uremic toxins. Nx; Nephrectomized rats, Nx+C; canagliflozin-treated Nx, Nx+T; tofogliflozin-treated Nx.*$p < 0.05$, **$p < 0.01$ versus the Sham group; †$p < 0.05$, ††$p < 0.01$ *versus* the Nx group; ‡$p < 0.05$ versus the Nx+C group ($n = 12$ per group)
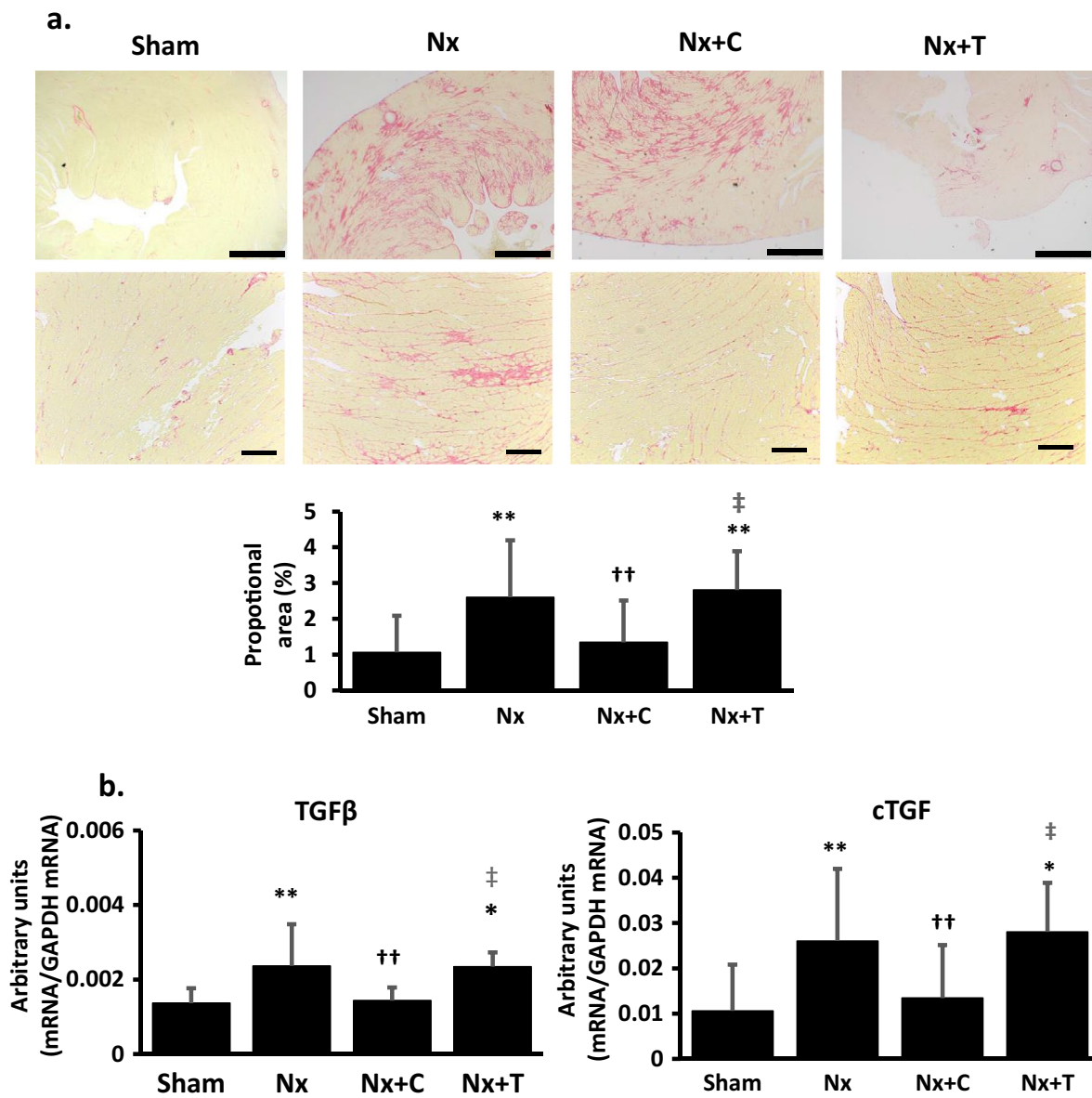
Fig. 5 Effect of tofogliflozin and canagliflozin on cardiac fibrosis. **a** Representative images of left ventricles stained using Picrosirius red (upper panel) and the proportions of the myocardium that were fibrotic (lower panel). Upper panel shows a photo of low-power field (scale bars; 1 mm) and lower panel shows a photo of high-power field (scale bars; 500 μm). The bar graph in the bottom represents propor-tion of the myocardium that was fibrotic. **b** Cardiac *Tgfb1* (left panel) and *Ctgf* (right panel) mRNA expression. Nx; Nephrectomized rats, Nx + C; canagliflozin-treated Nx, Nx + T; tofogliflozin-treated Nx *$p < 0.05$, **$p < 0.01$ versus the Sham group; ††$p < 0.01$ versus the Nx group, ‡$p < 0.05$ *versus* the Nx + C group ($n = 12$ per group)

to evert reno-protective effects for diabetic subjects [55, 56]. The short observation period in the present study is also the reason for the discrepant results to previous clinical trials. These negative results in the present study are consistent with the previous report [57, 58]. On the contrary, in the present study, canagliflozin slightly increased the urinary protein excretion in Nx rats, in which results were also unexpected. It is suspected that increased urinary volume by canagliflozin would activate RAS in the kidney and worsen

glomerular hypertension [59]. It would not be better to treat non-diabetic CKD patients with SGLT2 inhibitors without using combined RAS inhibitors.

However, canagliflozin ameliorated both the aortic wall thickening and cardiac interstitial fibrosis of the Nx rats. IS has been shown to induce oxidative stress in cardio-myocytes and to aggravate cardiac fibrosis [26, 27, 52, 60], and it has also been previously shown that CKD-induced cardiac fibrosis can be ameliorated by a reduction in the

circulating concentration of IS [26, 61]. In the present study, the high cardiac expression of *Tgfb1* and *Ctgf* in the Nx rats was ameliorated by treatment with canagliflozin, which suggests that canagliflozin ameliorates cardiac fibrosis by reducing the serum IS concentration and inhibiting the fibrogenic ROS-nuclear factor-κB-transforming growth factor β pathway. In addition, IS has been shown to induce oxidative stress in endothelial cells and promote aortic wall thickening [27–29]. Therefore, we believe that canagliflozin ameliorates the aortic wall thickening of the Nx rats by reducing their serum IS concentration. It can be deduced that in contrast to renal tissues which was subject to the direct ablation by nephrectomy, the cardiac tissue damages were indirect through the remote effects by renal insufficiency. Therefore, canagliflozin exerted the tissue protective effect.

In the present study, the cardiac fibrosis of the Nx rats was reduced by canagliflozin treatment but not by tofogliflozin treatment. This implies that the inhibition of SGLT1 may be the mechanism whereby canagliflozin has an anti-atherosclerotic effect in this non-diabetic model of CKD. There have been few reports of the effects of SGLT2 inhibitors in animal models of or patients with non-diabetic CKD. One previous study showed that the SGLT2 inhibitor dapagliflozin does not prevent proteinuria or a decline in GFR in non-diabetic Nx rats [57], which is consistent with the results of the present study. Recently, canagliflozin was also shown to alter the gut microbial composition and reduce the plasma concentrations of PCS and IS in mice with adenine-induced CKD [58]. In their paper, the authors hypothesized that the inhibition of SGLT1 by canagliflozin affects the intestinal environment and reduces the accumulation of uremic toxins. However, they did not study the cardiovascular effects of the drug, and so the present study is the first to show beneficial effects of a SGLT2 inhibitor on cardiovascular complications in a non-diabetic model of CKD. We conclude that canagliflozin may improve the long-term prognosis of patients with CKD by ameliorating their cardiac fibrosis and arthrosclerosis.

In conclusion, we have shown that the SGLT2 inhibitor canagliflozin protects the cardiovascular system of non-diabetic rats with CKD through its inhibition of SGLT1. The mechanism likely involves a reduction in the serum concentrations of gut-derived uremic toxins, secondary to an increase in the abundance of *Lactobacillus*. These findings suggest a novel therapeutic strategy for the cardiovascular complications of patients with CKD.

Declarations

Conflict of interest The authors have declared that no conflicts of interest exist.

Human and animal rights The animal studies were performed in accordance with the guidelines and regulations for animal experimentation of, and were approved by, the Keio University Animal Care and Use Committee (approval number KO 15069). Every effort was made to minimize the suffering of the rats.

References

1. Aronov PA, Luo FJ, Plummer NS, et al. Colonic contribution to uremic solutes. J Am Soc Nephrol. 2011;22:1769–76.
2. Kikuchi M, Ueno M, Itoh Y, Suda W, Hattori M. Uremic toxin-producing gut microbiota in rats with chronic kidney disease. Nephron. 2017;135:51–60.
3. Schepers E, Glorieux G, Vanholder R. The gut: the forgotten organ in uremia? Blood Purif. 2010;29:130–6.
4. Wong J, Piceno YM, Desantis TZ, Pahl M, Andersen GL, Vaziri ND. Expansion of urease- and uricase-containing, indole- and p-cresol-forming and contraction of short-chain fatty acid-producing intestinal microbiota in ESRD. Am J Nephrol. 2014;39:230–7.
5. Mutsaers HA, Stribos EG, Glorieux G, Vanholder R, Olinga P. Chronic kidney disease and fibrosis: the role of uremic retention solutes. Front Med (Lausanne). 2015;2:60.
6. Meijers BK, Evenepoel P. The gut-kidney axis: indoxyl sulfate, p-cresyl sulfate and CKD progression. Nephrol Dial Transplant. 2011;26:759–61.
7. Tan X, Cao X, Zou J, et al. Indoxyl sulfate, a valuable biomarker in chronic kidney disease and dialysis. Hemodial Int. 2017;21:161–7.
8. Hung SC, Kuo KL, Wu CC, Tarng DC. Indoxyl sulfate: a novel cardiovascular risk factor in chronic kidney disease. J Am Heart Assoc. 2017;6:161–7.
9. Vaziri ND, Wong J, Pahl M, et al. Chronic kidney disease alters intestinal microbial flora. Kidney Int. 2013;83:308–15.
10. Vaziri ND, Yuan J, Rahimi A, Ni Z, Said H, Subramanian VS. Disintegration of colonic epithelial tight junction in uremia: a likely cause of CKD-associated inflammation. Nephrol Dial Transplant. 2012;27:2686–93.
11. Vaziri ND, Yuan J, Norris K. Role of urea in intestinal barrier dysfunction and disruption of epithelial tight junction in chronic kidney disease. Am J Nephrol. 2013;37:1–6.
12. Yoshifuji A, Wakino S, Irie J, et al. Gut *Lactobacillus* protects against the progression of renal damage by modulating the gut environment in rats. Nephrol Dial Transplant. 2016;31:401–12.
13. Mafra D, Borges N, Alvarenga L, et al. Dietary components that may influence the disturbed gut microbiota in chronic kidney disease. Nutrients. 2019;11:496.
14. Koppe L, Mafra D, Fouque D. Probiotics and chronic kidney disease. Kidney Int. 2015;88:958–66.
15. Moraes C, Borges NA, Mafra D. Resistant starch for modulation of gut microbiota: promising adjuvant therapy for chronic kidney disease patients? Eur J Nutr. 2016;55:1813–21.

16. Kurosaki E, Ogasawara H. Ipragliflozin and other sodium-glucose cotransporter-2 (SGLT2) inhibitors in the treatment of type 2 diabetes: preclinical and clinical data. Pharmacol Ther. 2013;139:51–9.

17. Ohgaki R, Wei L, Yamada K, et al. Interaction of the sodium/glucose cotransporter (SGLT) 2 inhibitor canagliflozin with SGLT1 and SGLT2. J Pharmacol Exp Ther. 2016;358:94–102.

18. Sawada Y, Izumida Y, Takeuchi Y, et al. Effect of sodium-glucose cotransporter 2 (SGLT2) inhibition on weight loss is partly mediated by liver-brain-adipose neurocircuitry. Biochem Biophys Res Commun. 2017;493:40–5.

19. Ito S, Hosaka T, Yano W, et al. Metabolic effects of tofogliflozin are efficiently enhanced with appropriate dietary carbohydrate ratio and are distinct from carbohydrate restriction. Physiol Rep. 2018;6:e13642.

20. Kuriyama C, Xu JZ, Lee SP, et al. Analysis of the effect of canagliflozin on renal glucose reabsorption and progression of hyperglycemia in zucker diabetic fatty rats. J Pharmacol Exp Ther. 2014;351:423–31.

21. Sugano N, Wakino S, Kanda T, et al. T-type calcium channel blockade as a therapeutic strategy against renal injury in rats with subtotal nephrectomy. Kidney Int. 2008;73:826–34.

22. Oguma T, Nakayama K, Kuriyama C, et al. Intestinal sodium glucose cotransporter 1 inhibition enhances glucagon-like peptide-1 secretion in normal and diabetic rodents. J Pharmacol Exp Ther. 2015;354:279–89.

23. Kikuchi K, Itoh Y, Tateoka R, Ezawa A, Murakami K, Niwa T. Metabolomic search for uremic toxins as indicators of the effect of an oral sorbent AST-120 by liquid chromatography/tandem mass spectrometry. J Chromatogr B Analyt Technol Biomed Life Sci. 2010;878:2997–3002.

24. Kelly DJ, Zhang Y, Gow R, Gilbert RE. Tranilast attenuates structural and functional aspects of renal injury in the remnant kidney model. J Am Soc Nephrol. 2004;15:2619–29.

25. Wu LL, Cox A, Roe CJ, Dziadek M, Cooper ME, Gilbert RE. Transforming growth factor beta 1 and renal injury following subtotal nephrectomy in the rat: role of the renin-angiotensin system. Kidney Int. 1997;51:1553–67.

26. Lekawanvijit S, Kompa AR, Manabe M, et al. Chronic kidney disease-induced cardiac fibrosis is ameliorated by reducing circulating levels of a non-dialysable uremic toxin, indoxyl sulfate. PLoS ONE. 2012;7: e41281.

27. Yisireyili M, Shimizu H, Saito S, Enomoto A, Nishijima F, Niwa T. Indoxyl sulfate promotes cardiac fibrosis with enhanced oxidative stress in hypertensive rats. Life Sci. 2013;92:1180–5.

28. Dou L, Jourde-Chiche N, Faure V, et al. The uremic solute indoxyl sulfate induces oxidative stress in endothelial cells. J Thromb Haemost. 2007;5:1302–8.

29. Adijiang A, Goto S, Uramoto S, Nishijima F, Niwa T. Indoxyl sulphate promotes aortic calcification with expression of osteoblast-specific proteins in hypertensive rats. Nephrol Dial Transplant. 2008;23:1892–901.

30. Polidori D, Sha S, Mudaliar S, et al. Canagliflozin lowers postprandial glucose and insulin by delaying intestinal glucose absorption in addition to increasing urinary glucose excretion: results of a randomized, placebo-controlled study. Diabetes Care. 2013;36:2154–61.

31. Mei X, Zhang X, Wang Z, et al. Insulin sensitivity-enhancing activity of phlorizin is associated with lipopolysaccharide decrease and gut microbiota changes in obese and Type 2 diabetes (db/db) mice. J Agric Food Chem. 2016;64:7502–11.

32. Jiang Q, Kainulainen V, Stamatova I, Korpela R, Meurman JH. Lactobacillus rhamnosus GG in experimental oral biofilms exposed to different carbohydrate sources. Caries Res. 2018;52:220–9.

33. Stingley RL, Liu H, Mullis LB, Elkins CA, Hart ME. *Staphylococcus aureus* toxic shock syndrome toxin-1 (TSST-1) production and *Lactobacillus* species growth in a defined medium simulating vaginal secretions. J Microbiol Methods. 2014;106:57–66.

34. Christensen EG, Licht TR, Leser TD, Bahl MI. Dietary xylo-oligosaccharide stimulates intestinal bifidobacteria and lactobacilli but has limited effect on intestinal integrity in rats. BMC Res Notes. 2014;7:660.

35. Markowiak P, Slizewska K. Effects of probiotics, prebiotics, and synbiotics on human health. Nutrients. 2017;9:1021.

36. Azcarate-Peril MA, Ritter AJ, Savaiano D, et al. Impact of short-chain galactooligosaccharides on the gut microbiome of lactose-intolerant individuals. Proc Natl Acad Sci USA. 2017;114:E367–75.

37. Guida B, Germano R, Trio R, et al. Effect of short-term synbiotic treatment on plasma p-cresol levels in patients with chronic renal failure: a randomized clinical trial. Nutr Metab Cardiovasc Dis. 2014;24:1043–9.

38. Nakabayashi I, Nakamura M, Kawakami K, et al. Effects of synbiotic treatment on serum level of p-cresol in haemodialysis patients: a preliminary study. Nephrol Dial Transplant. 2011;26:1094–8.

39. Rossi M, Johnson DW, Morrison M, et al. SYNbiotics easing renal failure by improving gut microbiologY (SYNERGY): a protocol of placebo-controlled randomised cross-over trial. BMC Nephrol. 2014;15:106.

40. Skye SM, Hazen SL. Microbial modulation of a uremic toxin. Cell Host Microbe. 2016;20:691–2.

41. Gryp T, Vanholder R, Vaneechoutte M, Glorieux G. p-Cresyl sulfate. Toxins (Basel). 2017;9:52.

42. Lees HJ, Swann JR, Wilson ID, Nicholson JK, Holmes E. Hippurate: the natural history of a mammalian-microbial cometabolite. J Proteome Res. 2013;12:1527–46.

43. Sallee M, Dou L, Cerini C, Poitevin S, Brunet P, Burtey S. The aryl hydrocarbon receptor-activating effect of uremic toxins from tryptophan metabolism: a new concept to understand cardiovascular complications of chronic kidney disease. Toxins (Basel). 2014;6:934–49.

44. Zhu W, Stevens AP, Dettmer K, et al. Quantitative profiling of tryptophan metabolites in serum, urine, and cell culture supernatants by liquid chromatography-tandem mass spectrometry. Anal Bioanal Chem. 2011;401:3249–61.

45. Motojima M, Hosokawa A, Yamato H, Muraki T, Yoshioka T. Uremic toxins of organic anions up-regulate PAI-1 expression by induction of NF-kappaB and free radical in proximal tubular cells. Kidney Int. 2003;63:1671–80.

46. Owada S, Goto S, Bannai K, Hayashi H, Nishijima F, Niwa T. Indoxyl sulfate reduces superoxide scavenging activity in the kidneys of normal and uremic rats. Am J Nephrol. 2008;28:446–54.

47. Aldigier JC, Kanjanbuch T, Ma LJ, Brown NJ, Fogo AB. Regression of existing glomerulosclerosis by inhibition of aldosterone. J Am Soc Nephrol. 2005;16:3306–14.

48. Nangaku M. Chronic hypoxia and tubulointerstitial injury: a final common pathway to end-stage renal failure. J Am Soc Nephrol. 2006;17:17–25.

49. Heyman SN, Khamaisi M, Rosen S, Rosenberger C. Renal parenchymal hypoxia, hypoxia response and the progression of chronic kidney disease. Am J Nephrol. 2008;28:998–1006.

50. Ichii O, Otsuka-Kanazawa S, Nakamura T, et al. Podocyte injury caused by indoxyl sulfate, a uremic toxin and aryl-hydrocarbon receptor ligand. PLoS ONE. 2014;9: e108448.

51. Lin CJ, Wu V, Wu PC, Wu CJ. Meta-analysis of the associations of p-Cresyl sulfate (PCS) and indoxyl sulfate (IS) with cardiovascular events and all-cause mortality in patients with chronic renal failure. PLoS ONE. 2015;10: e0132589.

52. Ramezani A, Massy ZA, Meijers B, Evenepoel P, Vanholder R, Raj DS. Role of the gut microbiome in uremia: a potential therapeutic target. Am J Kidney Dis. 2016;67:483–98.

53. Katsumata H, Suzuki H, Ohishi A, Nakamoto H, Saruta T, Sakaguchi H. Effects of antihypertensive agents on blood pressure and the progress of renal failure in partially nephrectomized spontaneously hypertensive rats. Lab Invest. 1990;62:474–80.

54. Georgianos PI, Vaios V, Dounousi E, Salmas M, Eleftheriadis T, Liakopoulos V. Mechanisms for cardiorenal protection of SGLT-2 Inhibitors. Curr Pharm Des. 2021;27:1043–50.

55. Perkovic V, Jardine MJ, Neal B, et al. Canagliflozin and renal outcomes in Type 2 diabetes and nephropathy. N Engl J Med. 2019;380:2295–306.

56. Heerspink HJL, Stefánsson BV, Correa-Rotter R, et al. Dapagliflozin in patients with chronic kidney disease. N Engl J Med. 2020;383:1436–46.

57. Zhang Y, Thai K, Kepecs DM, Gilbert RE. Sodium-glucose linked cotransporter-2 inhibition does not attenuate disease progression in the rat remnant kidney model of chronic kidney disease. PLoS ONE. 2016;11: e0144640.

58. Mishima E, Fukuda S, Kanemitsu Y, et al. Canagliflozin reduces plasma uremic toxins and alters the intestinal microbiota composition in a chronic kidney disease mouse model. Am J Physiol Renal Physiol. 2018;315:F824–33.

59. Li L, Konishi Y, Morikawa T, et al. Effect of a SGLT2 inhibitor on the systemic and intrarenal renin-angiotensin system in subtotally nephrectomized rats. Pharmacol Sci. 2018;137(2):220–3.

60. Yang K, Xu X, Nie L, et al. Indoxyl sulfate induces oxidative stress and hypertrophy in cardiomyocytes by inhibiting the AMPK/UCP2 signaling pathway. Toxicol Lett. 2015;234:110–9.

61. Ali BH, Inuwa I, Al Za'abi M, et al. Renal and myocardial histopathology and morphometry in rats with adenine - induced chronic renal failure: influence of gum acacia. Cell Physiol Biochem. 2014;34:818–28.